New Chitosan-Silver Nanocomposites Containing N-Nicontinyl Phosphoric Triamide as an Antibacterial- Enhancer Additive

Oroujzadeh, Nasrin*[+]

Department of Chemical Technologies, Iranian Research Organization for Science and Technology (IROST), Tehran, I.R. IRAN

ABSTRACT: *Three new nanocomposite films of Chitosan/ Ag NPs / N-Nicontinyl phosphoric triamide, containing 3% Ag NPs and 0%, 5% and 10% phosphoric triamide were prepared and characterized by X-ray Powder Diffraction (XRD), Field Emission Scanning Electron Microscopy (FE-SEM), and Energy Dispersive X-ray Spectroscopy (EDS) analysis methods. The nanocomposite films were prepared using ultrasonic waves plus cross-linking the chitosan part of biofilms as the final process and the Ag NPs were synthesized according to the citrate reduction method. XRD graph of the three nanocomposites showed all the characteristic peaks of the phosphoric triamide, Ag NPs, and chitosan, indicating the fact that the preparing process has not made any changes in the phases of the nanocomposites components. All the SEM micrographs and EDS analysis results confirmed the desired structures. In vitro antibacterial activities of the nanocomposite were tested against two Gram-positive bacteria: Staphylococcus aureus (S. aureus), Bacillus cereus (B. cereus) and two Gram-negative bacteria: Escherichia coli (E. coli), Pseudomonas aeruginosa (P. aeruginosa) in Brain-Heart Infusion (BHI) medium. Results revealed that the nanocomposite films, containing the phosphoric triamide additive, have better antibacterial effects than the one without this compound. Also, the antibacterial activity of the biofilms depends on the dosage of the phosphoric triamide and increases by raising the percentage of the additive in the structure of biofilms.*

KEYWORDS: *Chitosan; Ag NPs; Nanocomposite; Phosphoric triamide additive; Antibacterial.*

INTRODUCTION

Recently, a growing interest has been observed in biocidal compounds based on biopolymers, especially chitosan. Owing to the biodegradable, biocompatible, and non-toxic nature of chitosan, several biomedical applications have been reported for this biopolymer, such as drug delivery [1], wound healing [2], and gene delivery [3,4]. The chitosan-based antibacterial films can be used on medical devices to enhance their bactericidal efficiency and to reduce infections [5–9]. In the last Few years, chitosan/Ag nanocomposites have been very attractive due to their antibacterial behavior [10–13]. The investigation of antibacterial properties of crosslinked nanocomposites chitosan/poly (ethylene glycol) (PEG) /Ag/ZnO has shown that they have potential applications as burn and wound dressings [14]. There are also some reports about good antibacterial activities of a new aminoacid–chitosan/Ag nanocomposite film [15] and of porous chitosan films impregnated with silver NPs [16].

** To whom correspondence should be addressed.*
+ E-mail: n_oroujzadeh@irost.ir
1021-9986/2020/4/1-9 9/$/5.09

Among metal nanoparticles, Ag NPs have attracted much attention due to their high biocompatibility, antibacterial activity, electrical and optical properties and consequently potential applications in sensors, biosensors, and electronic equipment [17–21].

Synthesis of various Ag nanomaterials has been an active research area in recent years, it has been found that the physicochemical properties of Ag nanomaterials depend on their shape, size, and surface capping agent [22, 23].

In recent decay, phosphoramidic compounds have been very attractive due to their noble properties. This class of materials has revealed valuable potential for various applications such as catalysts for different chemical reactions [24,25], anticancer prodrugs [10, 26, 27] and inhibitors for butyrylcholinesterase [28], cholinesterase [29,30], and urease [31, 32] enzymes.

The biocidal property of phosphoramides is also so well known that they are used as insecticides and pesticides in agriculture [33,34]. In our late researches [35,36] we prepared some new chitosan-based nanocomposites, containing some dosages of silver nanoparticles and phosphoramide derivatives, and we showed that these nanocomposites have acceptable antibacterial properties.

Here, following our previous works [35,36], three new nanocomposite films of chitosan/AgNPs/N-Nicontinyl phosphoric triamide were prepared, using the crosslinking method, which contains 3% of silver nanoparticles plus 0%, 5%, and 10 % of the phosphoric triamide additive. X-ray Powder Diffraction (XRD), Field Emission Scanning Electron Microscopy (FE-SEM) and Energy Dispersive X-ray Spectroscopy (EDS) methods were used for characterization and confirmation of the frameworks. Then, the *in vitro* antibacterial effects of the prepared nanocomposites were evaluated on four bacteria including two Gram-positive: Bacillus cereus (B. cereus), Staphylococcus aureus (S. aureus) and two Gram-negative: Pseudomonas *aeruginosa (P. aeruginosa*), *Escherchia coli* (E. coli) in Brain-Heart Infusion (BHI) medium and the effect of the phosphoric triamide additive dosage on the antibacterial activity of the nanocomposite was studied.

EXPERIMENTAL SECTION

Materials

Phosphorpentachloride(PCl_5), tert-butyl amine, Carbon tetrachloride(CCl_4), Acetonitrile, Silver nitrate, Sodium citrate, Ethanol, Acetic acid, Nicotinamide and distilled water obtained from Merck Co. Glutaraldehyde (25 wt% in water) obtained from Daejong Co. and high molecular weight Chitosan was purchased from Loba Chemie Pvt. Ltd. All compounds were used without any more purification.

Synthesis

Synthesis of N-Nicontinyl phosphoric triamide (PT): $C_5H_4NC(O)NHP(O)[NHC(CH_3)_3]_2$

This compound was synthesized according to the literature method [37]. Briefly, to a mixture of N-Nicotinyl phosphoramidic dichloride (1 mmol), tert-Butylamine (4 mmol) and Acetonitrile were added at 0 ◦C. After 8 h, the precipitate was filtered; the residue was washed with distilled water and was dried at 25 ◦C to obtain the final product.

Synthesis of Ag nanoparticles

The Ag nanoparticles were synthesized by the citrate reduction method [29]. An aqueous solution (2 mmol) of silver nitrate was added to an aqueous sodium citrate solution (1 mmol), under atmospheric conditions. To avoid a light-induced reduction of Ag, the reaction flask was heated in a dark environment, to about 140 C for 6 h. Then, it was cooled to room temperature and the Ag nanoparticles were filtered and dried after washing with distilled water, several times.

Preparation of Chitosan/ Ag NPs/ Phosphoric triamide (PT) nanocomposite films

For preparing the nanocomposite, at first, 0.5 g of chitosan powder was dispersed in 5 mL of distilled water and 3 mL acetic acid was added to the mixture. Next, the mixture was placed in an ultrasonic bath for 2 h to yield a homogenous brown viscose gel. Then, Phosphoric triamide (PT) powder (0, 5, and 10% w/w of chitosan, for the films **NC1**, **NC2,** and **NC3** respectively) was dissolved in ethanol, added to the chitosan, and placed into the ultrasonic bath for 30 min. After that, Ag NPs (3% w/w of chitosan) was added to the chitosan/ PT flask and placed in the ultrasonic bath for 30 min. The homogenous mixtures were then poured into proper plates and were allowed to be dried. Finally, the prepared films were put in a desiccator containing glutar aldehyde steam with the pressure of 0.5 atm for 24 hours,

for the crosslinking of chitosan and obtaining the desired nanocomposite films.

Instrumentations

The phase analysis of the fabricated framework was done by an X-Ray Diffraction (XRD) diffractometer, model: Equinox 3000, Intel Co. The micrographs and elemental analysis were obtained from the Field Emission Scanning Electron Microscopy (FE-SEM) model: Mira II, Tescan Co., and Energy Dispersive Spectroscopy (EDS) model: Mira II, Tescan Co. instruments. Ultrasonic bath, model: S 4000, Misonix Co. with output power:600W was used in the preparation process.

In Vitro antibacterial test

Filter paper disk method was used to evaluate the *in vitro* antibacterial activities of the prepared films [36], with the disk diameter of 6.5 mm. The bacteria were cultured in BHI medium. About 0.005 g of each film was used in each test. The thickness of the BHI medium was kept equal in all Petri dishes. Four bacteria including two Gram-positive (S. aureus, B. cereus) and two Gram-negative bacteria (E. coli, P. aeruginosa) were examined. The disks were incubated at 37˚ C for 24 h. The inhibition zone of growth was measured and the average of three diameters was calculated for each sample (Table 1).

RESULTS AND DISCUSSION

FT-IR Spectroscopy

The FT-IR spectroscopy was applied to confirm the main functional groups of the prepared phosphoric triamide structure. Results showed good accordance with the ones in the reference (Table 1). The small differences between the frequencies are because of the dissimilarity of the instruments and using FT-IR instead of IR.

FT-IR spectroscopy was also used for checking the main functional groups of the fabricated nanocomposites. But, as Chitosan was the main phase of the nanocomposites, the broad intense bands of Chitosan covered the phosphoramide bands, in all cases.

X-Ray Diffraction (XRD) analysis

The X-Ray Diffraction (XRD) method was used to characterize the materials and phases. XRD pattern of each nanocomposite components (Ag NPs, Chitosan, and phosphoric triamide) are given in Fig. 1. The strong diffraction pattern of Ag nanoparticles is related to the hkl values of (1 1 1), (2 0 0), (2 2 0), (3 1 1) and (2 2 2) planes, that matches with the standard JCPDS No. [00 – 087– 0597].

The Phosphoric Triamide (**PT**) is a newly synthesized compound and its XRD pattern is reported here for the first time. The XRD graph of chitosan includes all the characteristics peak of chitosan, reported in the literature [15,38]. As it can be seen in Fig. 1, owing to their high crystallinity, Ag NPs and Phosphoric Triamide (**PT**) represent sharp peaks; but the chitosan film shows a broad pattern, which refers to its amorphous polymeric structure.

XRD patterns of the three fabricated nanocomposite films **NC1**, **NC2,** and **NC3** are shown in Fig. 2. Comparing Figs. 1 and 2 indicates that all the characteristic peaks of **PT**, Ag NPs, and chitosan are observed in the XRD patterns of **NC1**, **NC2,** and **NC3**, which confirms that the mixing process has not made any changes in the phases of the nanocomposites components. The intensity of some of components picks have been changed, which is due to the using of ultrasonic waves in the mixing process.

FE-SEM & EDS

To study the surface morphology of the nanocomposites and measuring the average particle size of the Ag NPs, the FE-SEM micrographs were obtained and represented in Figs. 3 and 4. FE-SEM micrograph of Ag NPs indicates that the average particle size of Ag NPs is about 80-90 nm and most of these ultrafine particles have been accumulated with each other (Fig. 3).

Fig. 4 shows the FE-SEM micrographs of nanocomposites **NC1**, **NC2,** and **NC3**, containing: Chitosan, Ag (3%w of chitosan) plus 0%, 5%, and 10% (weight of chitosan) phosphoric triamide, respectively. The presence of Ag NPs can be obviously observed in these images. A comparison between the micrograph of **NC1** with **NC2** and **NC3** films indicates that **NC2** and **NC3** have a better surface with a more homogenous dispersion of smaller Ag nanoparticles. This could be due to the more stirring time under ultrasonic waves for **NC2** and **NC3**, owing to the step of adding the phosphoric triamide (**PT**) additive, which **NC1** did not have.

Table 1: Main FT-IR bands for PT in comparison to the reference.

$\nu_{(C=O)}$ $(cm)^{-1}$	$\nu_{(P=O)}$ $(cm)^{-1}$	$\nu_{pyridine}$ $(cm)^{-1}$	$\delta_{pyridine}$ $(cm)^{-1}$	$\gamma_{pyridine}$ $(cm)^{-1}$	Ref.
1669	1189	1579	734	592	[37]
1672	1182	1580	740	594	Present work

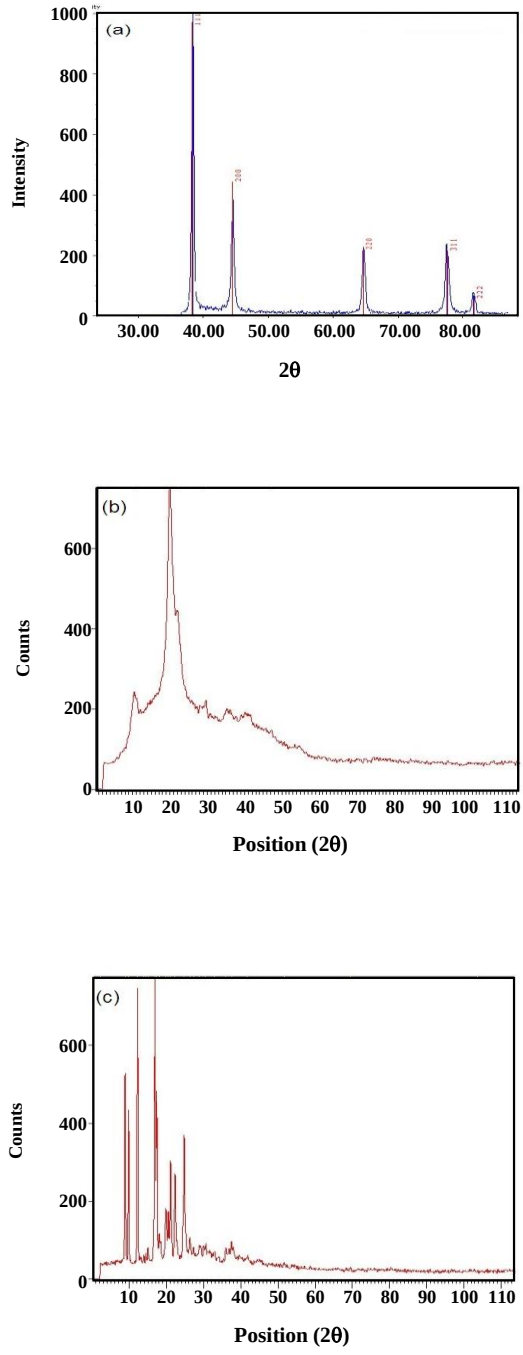

Fig. 1: XRD pattern of Ag Nps(a) Chitosan(b) and Phosphoric triamide(c).

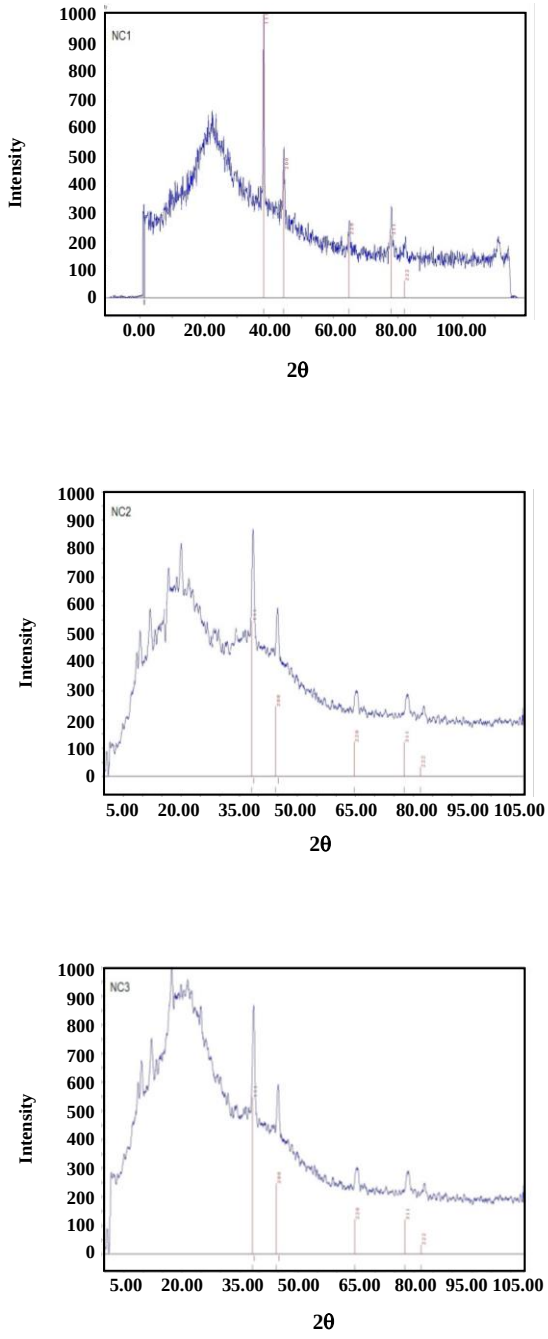

Fig. 2: XRD pattern of Chitosan / 3%Ag nanocomposites containing different dosages of phosphoric triamide additive: 0% (NC1), 5% (NC2) and 10% (NC3).

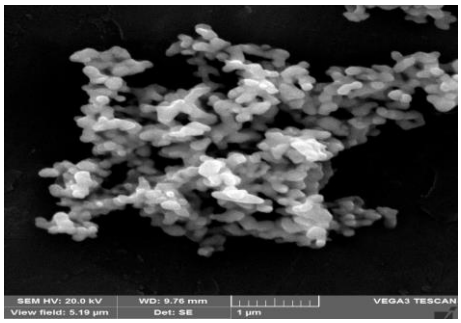

Fig. 3: FE-SEM micrographs of Ag nanoparticles.

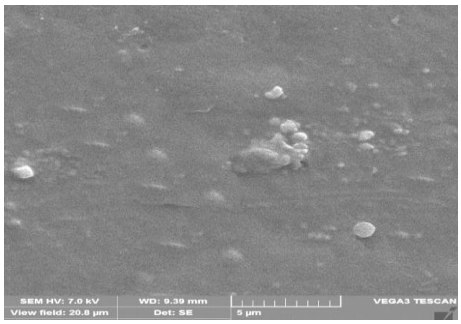

NC1

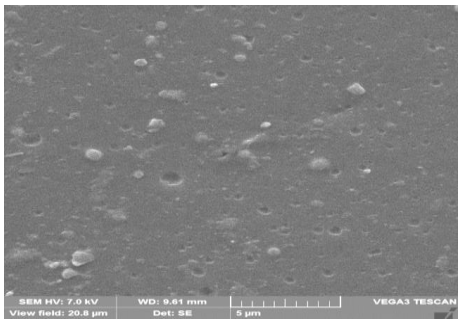

NC2

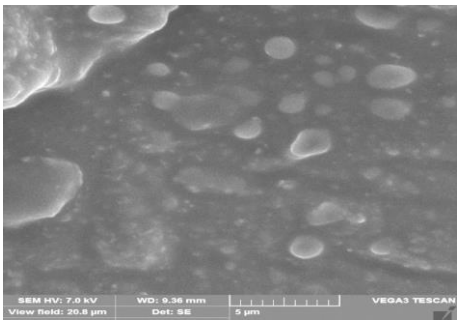

NC3

Fig. 4: FE-SEM micrographs of nanocomposites NC1, NC2, and NC3.

To confirm the presence of all initial components and all their elements in the nanocomposites framework Energy Dispersive Spectroscopy (EDS) was applied. EDS analysis of **NC1**, **NC2,** and **NC3**, containing 0%, 5%, and 10% of **PT**, are shown in Fig. 5, which verifies the existence of all the designed parts within the nanofilms and confirms the desired percentages of the elements. The presence of the phosphoric triamide (**PT**) additive in **NC2** and **NC3** can also be obviously detected by observing the Phosphorus element in their EDS (Fig. 5).

Antibacterial Activity

The *in vitro* antibacterial activities of nanocomposite **NC1**, **NC2,** and **NC3** were tested against four bacteria: two gram-positive (B. cereus, S. aureus), and two gram-negative (P. aeruginosa, E. coli). For all the three nanocomposites the inhibition zone of growth, which specifies the amount of inhibitory effect of the compounds on the growth of the bacteria, was measured for all the four bacteria. Each test was repeated for at least 3 times and the average amount of the results were summarized in Table 2.

The antibacterial results of our recently published similar nanocomposites were also listed in Table 1. As it can be seen from the table, all the three nanocomposites of the present work (**NC1** –**NC3**) have biocidal effects on all the four bacteria and the test results are in good agreement with those of previously reported similar frameworks [35,36]. It can be found out that the antibacterial activity of all listed nanocomposites (**NC1** –**NC7**) against B.cereus and P.aeruginosa is stronger than that against S.aureus and E.coli. A comparison between the inhibition zones of the newly fabricated films (**NC1** –**NC3**) indicates that the nanocomposites **NC2** and **NC3**, which contain the phosphoric triamide (**PT**) additive, have stronger antibacterial activity, against all four bacteria, than the one without this phosphoric triamide (**NC1**). Such result is also observed for other reported nanocomposites (**NC4** vs. **NC5)** and **(NC4** vs. **NC5)** and does not depend on the percentages of Ag Nps and the structure of the phosphoric triamide, confirming the good antibacterial enhancing property of these two phosphoric triamide additives (**PT** and **NHE**).

Moreover, comparing the antibacterial results of **NC1**, **NC2,** and **NC3**, about all the four bacteria, shows that the antibacterial property of these three nanocomposites

Table 2: The inhibition zone (mm) measured for the antibacterial activities.

Nanocomposite \ Bacteria	Gram Negative		Gram Positive		Ref.
	P. aeruginosa 1074	E. coli 1330	S. areous 1113	B. cereus 1254	*
Chitosan / 3% Ag NPs (NC1)	11.14± 0.49	8.01± 0.41	7.93± 0.29	11.08± 0.46	*
Chitosan /3% Ag NPs /5% PT (NC2)	14.28± 0.44	8.54± 0.33	8.70± 0.34	13.14± 0.38	*
Chitosan /3% Ag NPs /10% PT (NC3)	16.87± 0.36	9.53± 0.45	9.01± 0.37	16.79± 0.44	*
Chitosan / 7% Ag NPs (NC4)	11.99± 0.54	8.61± 0.49	8.47± 0.58	12.02± 0.48	[35]
Chitosan /7% Ag NPs /5% NHE** (NC5)	13.16± 0.42	10.45± 0.47	10.28± 0.51	13.53± 0.46	[35]
Chitosan/ 10% Ag NPs (NC6)	12.78± 0. 47	9.33± 0.57	9.11± 0.55	12.42± 0.51	[36]
Chitosan/ 10%Ag NPs/ 5% PT (NC7)	17.18± 0.55	14.05± 0.48	10.52± 0.47	12.61± 0.43	[36]

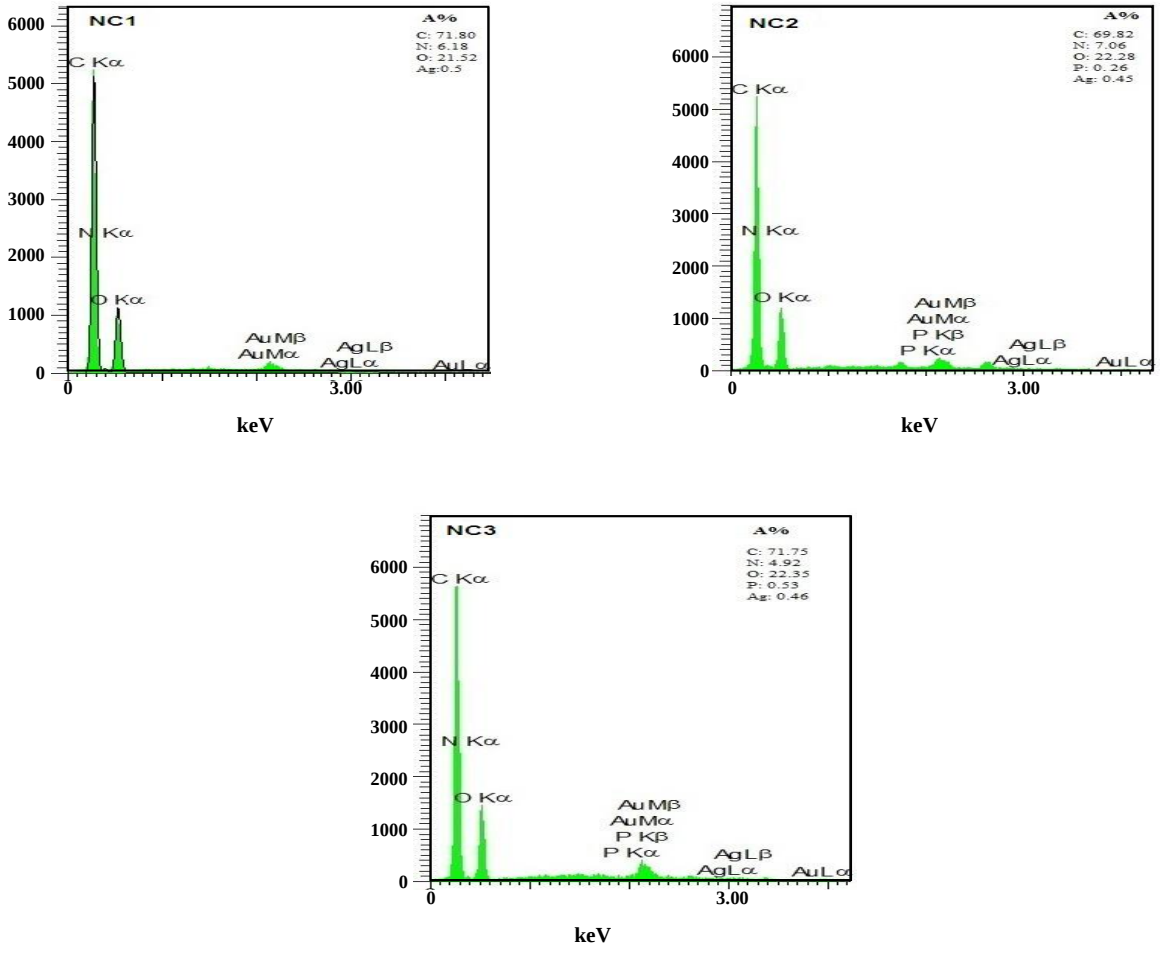

Fig. 5: EDS of nanocomposites NC1, NC2 and NC3.

depends on the dosage of the phosphoric triamide (**PT**) and increases by raising the percentage of this additive in the nanocomposites structures.

CONCLUSIONS

To study the effect of an additive on the antibacterial activity of a chitosan/Ag NPs, three new nanocomposite films were prepared, using the crosslinking method: Chitosan/3%Ag NPs (**NC1**), Chitosan/3%Ag NPs/5%PT (**NC2**) and Chitosan /3% Ag NPs /10% PT (**NC3**) where the additive **PT** was a N-Nicotinyl phosphoric triamide with the formula: $C_5H_4NC(O)NHP(O)[NHC(CH_3)_3]_2$. The desired nanoparticles and nanocomposites were characterized and confirmed by XRD, FE-SEM, and EDS. The *in vitro* antibacterial test against two Gram-negative (P. aeruginosa, E. coli) and two Gram-positive (B. cereus, S. aureus) bacteria indicated that the phosphoric triamide additive (**PT**) increases the antibacterial activity of the nanocomposite against all the four different bacteria and this increase are dosage-dependent to the additive.

Acknowledgments

All supports of the Iranian Research Organization for Science and Technology (IROST) are gratefully acknowledged.

Received : Dec. 18, 2018 ; Accepted :Apr. 29, 2019

REFERENCES

[1] Park J.H., Saravanakumar G., Kim K., Kwon I.C., Targeted Delivery of Low Molecular Drugs Using Chitosan and Its Derivatives, *Adv. Drug Delivery Rev.*, **62**(1): 28-41 (2010).

[2] Ueno H., Mori T., Fujinaga T., Topical Formulations and Wound Healing Applications of Chitosan, *Adv. Drug Delivery Rev.*, **52**(2): 105-115 (2001).

[3] Yoo H.S., Lee J.E., Chung H., Kwon I.C., Jeong S.Y., Self-assembled Nanoparticles Containing Hydrophobically Modified Glycol Chitosan for Gene Delivery, *J. Controlled Release*, **103**(1): 235-243 (2005).

[4] Chan P., Kurisawa M., Chung J.E., Yang Y.-Y., Synthesis and Characterization of Chitosan-g-Poly(ethylene glycol)-folate as a Non-Viral Carrier for Tumor-Targeted Gene Delivery, *Biomaterials*, **28**(3): 540-549 (2007).

[5] Bratskaya S., Marinin D., Simon F., Synytska A., Zschoche S., Busscher H.J., Jager D., Van der Mei H., Adhesion and Viability of Two Enterococcal Strains on Covalently Grafted Chitosan and Chitosan/κ-Carrageenan Multilayers, *Biomacromolecules* **8**(9): 2960-2968 (2007).

[6] Li J., Zivanovic S., Davidson P.M., Kit K., Production and Characterization of Thick, Thin and Ultra-Thin Chitosan/PEO Films, *Carbohydr. Polym.*, **83**(2): 375-382 (2011).

[7] Hsu S.-H., Wang M.-C., Lin J.-J., Biocompatibility and Antimicrobial Evaluation of Montmorillonite/Chitosan Nanocomposites, *Appl. Clay Sci.*, **56**: 53-62 (2012) .

[8] Han J., Zhou Z., Yin R., Yang D., Nie J., Alginate–Chitosan/Hydroxyapatite Polyelectrolyte Complex Porous Scaffolds: Preparation and Characterization, *Int. J. Biol. Macromol.*, **46**(2): 199-205 (2010).

[9] Yamane S., Iwasaki N., Majima T., Funakoshi T., Masuko T., Harada K., Minami A., Monde K., Nishimura S.-I., Feasibility of Chitosan-Based Hyaluronic Acid Hybrid Biomaterial for a Novel Scaffold in Cartilage Tissue Engineering, *Biomaterials*, **26**(6): 611-619 (2005).

[10] Hu L., Wu X., Han J., Chen L., Vass S. O., Browne P., Hall B.S., Bot C., Gobalakrishnapillai V., Searle P. F., Synthesis and Structure-Activity Relationships of Nitrobenzyl Phosphoramide Mustards as Nitroreductase-Activated Prodrugs, *Bioorg. Med. Chem. Lett.*, **21**(13): 3986-399 (2011).

[11] Pinto R. J., Fernandes S.C.M, Freire C. S., Sadocco P., Causio J., Neto C. P., Trindade T., Antibacterial Activity of Optically Transparent Nanocomposite Films Based on Chitosan or Its Derivatives and Silver Nanoparticles, *Carbohydr. Res.*, **348**: 77-83 (2012).

[12] Wang B.-L., Liu X.-S., Ji Y., Ren K.-F., Ji J., Fast and Long-Acting Antibacterial Properties of Chitosan-Ag/polyvinylpyrrolidone Nanocomposite Films, *Carbohydr. Polym.*, **90**(1): 8-15 (2012).

[13] Sanpui P., Murugadoss A., Prasad P.D., Ghosh S.S., Chattopadhyay A., The Antibacterial Properties of a Novel Chitosan–Ag-Nanoparticle Composite, *Int. J. Food Microbiol.*, **124**(2):142-146 (2008).

[14] Liu Y., Kim H.-I., Characterization and Antibacterial Properties of Genipin-Crosslinked Chitosan/Poly (ethylene glycol)/ZnO/Ag nanocomposites, *Carbohydr. Polym.*, **89**(1):111-116 (2012).

[15] Srivastava R., Tiwari D.K., Dutta P.K., 4-(Ethoxycarbonyl) Phenyl-1-amino-oxobutanoic Acid–Chitosan Complex as a New Matrix for Silver Nanocomposite Film: Preparation, Characterization and Antibacterial Activity, *Int. J. Bio.l Macromol*, **49** (5): 863-870 (2011).

[16] Vimala K., Mohan Y.M., Sivudu K.S., Varaprasad K., Ravindra S., Reddy N.N., Padma Y., Sreedhar B., MohanaRaju K., Fabrication of Porous Chitosan Films Impregnated with Silver Nanoparticles: a Facile Approach for Superior Antibacterial Application, *Colloids Surf., B* **76** (1): 248-258 (2010).

[17] Kango S., Kalia S., Celli A., Njuguna J., Habibi Y., Kumar R., Surface Modification of Inorganic Nanoparticles for Development of Organic-Inorganic Nanocomposites—A Review, *Prog. Polym. Sci.*, **38** (8): 1232-1261 (2013).

[18] Liu J., Jiang G., "Silver Nanoparticles in the Environment", Springer (2015).

[19] Schröfel A., Kratošová G., Šafařík I., Šafaříková M., Raška I., Shor L.M., Applications of Biosynthesized Metallic Nanoparticles–A Review, *Acta Biomater.*, **10**(10): 4023-5042 (2014).

[20] Fathalipour S., Pourbeyram S., Sharafian A., Tanomand A., Azam P., Biomolecule-Assisted Synthesis of Ag/reduced Graphene Oxide Nanocomposite with Excellent Electrocatalytic and Antibacterial Performance, *Mater. Sci. Eng.*, **75**: 742-751 (2017).

[21] Wang W., Zhang H., Tian C., Meng X., Numerical Experiments on Evaporation and Explosive Boiling of Ultra-Thin Liquid Argon Film on Aluminum Nanostructure Substrate, *Nanoscale Res. Lett.*, **10**(1):158- (2015).

[22] Wiley B., Sun Y., Mayers B., Xia Y., Shape-Controlled Synthesis of Metal Nanostructures: the Case of Silver, *Chem. Eur. J.*, **11** (2): 454-463 (2005).

[23] Rao C., Kulkarni G., Thomas P.J., Edwards P.P., Size-Dependent Chemistry: Properties of Nanocrystals, *Chem. Eur. J.*, **8** (1): 28-35 (2002).

[24] Sai M., Yamamoto H., Chiral Brønsted Acid as a True Catalyst: Asymmetric Mukaiyama Aldol and Hosomi–Sakurai Allylation Reactions, *J. Am. Chem. Soc.*, **137**(22):7091-7094 (2015).

[25] Nishikawa Y., Nakano S., Tahira Y., Terazawa K., Yamazaki K., Kitamura C., Hara O., Chiral Pyridinium Phosphoramide as a Dual Brønsted Acid Catalyst for Enantioselective Diels–Alder Reaction, *Org. Lett.*, **18**(9): 2004-2007 (2016).

[26] Jiang Y., Hu L., Peptide Conjugates of 4-Aminocyclophosphamide as Prodrugs of Phosphoramide Mustard for Selective Activation by Prostate-Specific Antigen (PSA), *Bioorganic. Med. Chem.*, **21**(23): 7507-7514 (2013).

[27] Rao K.K., Reddy P.R., Lee Y.-I., Kim C., Synthesis and Characterization of Chitosan–PEG–Ag Nanocomposites for Antimicrobial Application, *Carbohydr. Polym.*, **87**(1): 920-925 (2012).

[28] Gholivand K., Abdollahi M., Mojahed F., Alizadehgan A.M., Dehghan G., Acetylcholinesterase/ Butyrylcholinesterase Inhibition Activity of Some New Carbacylamidophosphate Derivatives, *J. Enzym. Inhib. Med. Ch.*, **24**(2): 566-576 (2009).

[29] Gholivand K., Alizadehgan A.M., Mojahed F., Dehghan G., Mohammadirad A., Abdollahi M., Some New Carbacylamidophosphates as Inhibitors of Acetylcholinesterase and Butyrylcholinesterase, *Z. Naturforsch. C.*, **63**(3-4): 241-250 (2008).

[30] Gholivand K., Valmoozi A.A., Bonsaii M., Synthesis, Biological Evaluation, QSAR Study and Molecular Docking of Novel N-(4-amino carbonylpiperazinyl)(thio) phosphoramide Derivatives as Cholinesterase Inhibitors, *Pestic. Biochem. Phys.*, **112**:40-50 (2014).

[31] Akgür S.A., Öztürk P., Solak I., Moral A. R., Ege B., Human Serum Paraoxonase (PON1) Activity in Acute Organophosphorous Insecticide Poisoning, *Forensic Sci. Int.*, **133**(1): 136-140 (2003).

[32] Zou X.J., Jin G.Y., Zhang Z.X., Synthesis, Fungicidal Activity, and QSAR of Pyridazinonethiadiazoles., *J. Agric. Food. Chem.*, **50**(6): 1451-1454 (2002).

[33] Wing K.D., Glickman A.H., Casida J.E., Phosphorothiolate Pesticides and Related Compounds: Oxidative Bioactivation and Aging of the Inhibited Acetylcholinesterase, *Pestic. Biochem. Physiol.*, **21**(1): 22-30 (1984).

[34] Miyamoto T., Kasagami T., Asai M., Yamamoto I., A Novel Bioactivation Mechanism of Phosphoramidate Insecticides, *Pestic. Biochem. Physiol.*, **63**(3): 151-162 (1999).

[35] Oroujzadeh N., New Chitosan/Ag/Carbacylamidophosphate Nanocomposites: Preparation and Antibacterial Study, *Adv.Environ.Technol. (AET)*, In press.

[36] Oroujzadeh N., Rezaei Jamalabadi S., New Nanocomposite of N-Nicotinyl, N′, N″-bis (tert-butyl) Phosphorictriamide Based on Chitosan: Fabrication and Antibacterial Investigation, *Phosphorus.Sulfur*, **191**(11-12): 1572-1573 (2016).

[37] Gholivand K., Oroujzadeh N., Afshar F., New Organotin (IV) Complexes of Nicotinamide, Isonicotinamide and Some of their Novel Phosphoric Triamide Derivatives: Syntheses, Spectroscopic Study and Crystal Structures, *J. Organomet. Chem.*, **695**(9): 1383-1391 (2010).

[38] Wang X., Du Y., Yang J., Wang X., Shi X., Hu Y., Preparation, Characterization and Antimicrobial Activity of Chitosan/Layered Silicate Nanocomposites, *Polymer*, **47**(19): 6738-6744 (2006).